EFFECT OF GEOMETRICAL ARRANGEMENT ON EXPERIMENTAL QUANTITIES IN PRIMARY PROCESSES OF PHOTOSYNTHESIS

V. KAPSA, O. BILEK and L. SKALA

Faculty of Mathematics and Physics, Charles University, 121 16 Prague 2, Czechoslovakia

Received 5 May 1986; in final form 2 June 1986

The effect of the number of antenna chlorophyll a molecules, their orientation and the dimensions of the reaction center on experimental quantities in a model of the antenna core based on the Pauli master equation is investigated. Results of numerical calculations, as well as analytic expressions for observables applicable from a few picoseconds after the excitation are given and discussed. The effect decreases with increasing time and from a few picoseconds it is very small.

1. Introduction

Most of the chlorophyll a (Chl) molecules in the photosystem of green plants serve as antenna for harvesting photons. Only a small part of the Chl forms – together with proteins – a large complex reaction center (RC) in which the excitation energy is transformed into electrochemical energy. The quantum yield of the energy transfer to the RC is very high.

The excitation energy transfer has been investigated in a number of experimental and theoretical works (see e.g. refs. [1–8]). In refs. [4–6], the random-walk method (RWM) was used to estimate the efficiency of the transfer for different configurations of the photosynthetic unit. The most favourable configuration was the one requiring the smallest number of RWM steps to transfer the excitation energy to the RC with a given probability. The shortcoming of using RWM in this field is that (a) it does not describe processes in real time, (b) it does not directly give observables, (c) the efficiency of the transfer should be estimated from the corresponding quantum yield rather than from the abovementioned criterion.

For these reasons, we use the Pauli master equation (PME) [9] in this work. Solving the PME for the probabilities of finding the excitation at different system levels, we can directly calculate the real time evolution of observables. Our approach is the same as in ref. [7] including the same intramolecular rate constants and the use of the Förster model for the intermolecular ones. In contrast to ref. [7], however, we investigate the effect of the number of antenna Chl molecules, their orientation and the dimensions of the RC on observables. At the same time, we present analytic expressions for these quantities which are applicable from a few picoseconds after the end of the excitation and we make appropriate physical conclusions.

2. Model

The singlet S_0, S_1 and triplet T_1 energy levels are considered both for the antenna Chl molecules and the RC represented by the so-called special pair. Since the energy transfer amongst the T_1 antenna levels is not considered here we may introduce a single T_1 level common to all the antennas. Analogously, we introduce two common S_0 antenna levels for $S_1 \rightarrow S_0$ and $T_1 \rightarrow S_0$ transitions, respectively. The same approach is used for the S_0 level of the RC (see fig. 1). This formal approach is very useful from the point of view of the numerical and analytical calculation of observables. The energy transferred to the RC is captured by the virtual charge-transfer level (CT). The intramolecular rate constants are determined from the spectroscopic data on monomeric chlorophyll a in diethylether and the intermolecular ones are calculated from the Förster formula [10] for a Förster radius of $R_0 = 6.4$ nm and the fluorescence

0 009-2614/86/$ 03.50

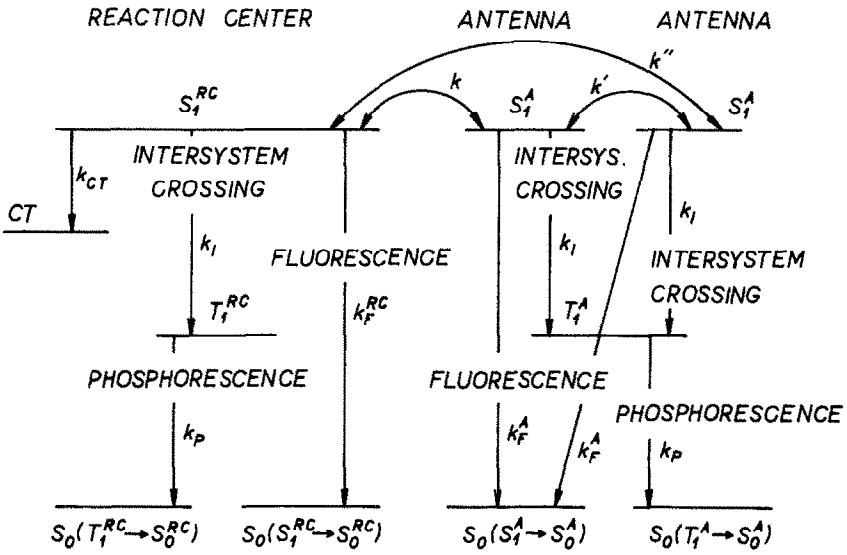

Fig. 1. Scheme of the levels and rate constants. Only the reaction center P680 (RC) and two antennas C678 are shown. S_0 ($S_1^{\lambda} \rightarrow S_0^{\lambda}$) and S_0 ($T_1^{\lambda} \rightarrow S_0^{\lambda}$) in the antenna system are two levels corresponding to the indicated transitions common to all the antennas. The same notation is used for the RC. Similarly, the T_1^{λ} level in the antenna system is also a single level common to all the antennas. The intramolecular rate constants are the same as in ref. [7]. $k_F^{\lambda} = 6.7 \times 10^7\ s^{-1}$, $k_I = 1.34 \times 10^8\ s^{-1}$, $k_F^{RC} = 1.34 \times 10^8\ s^{-1}$, $k_P = 5.9 \times 10^2\ s^{-1}$, $k_{CT} = 3.3 \times 10^{11}\ s^{-1}$. Here, the following notation is used. F, fluorescence; P, phosphorescence; I, intersystem crossing; A, antenna; RC, reaction center; CT, charge transfer level. The intermolecular rate constants k, k', k'' are calculated from the Förster formula for the Förster radius $R_0 = 6.4$ nm.

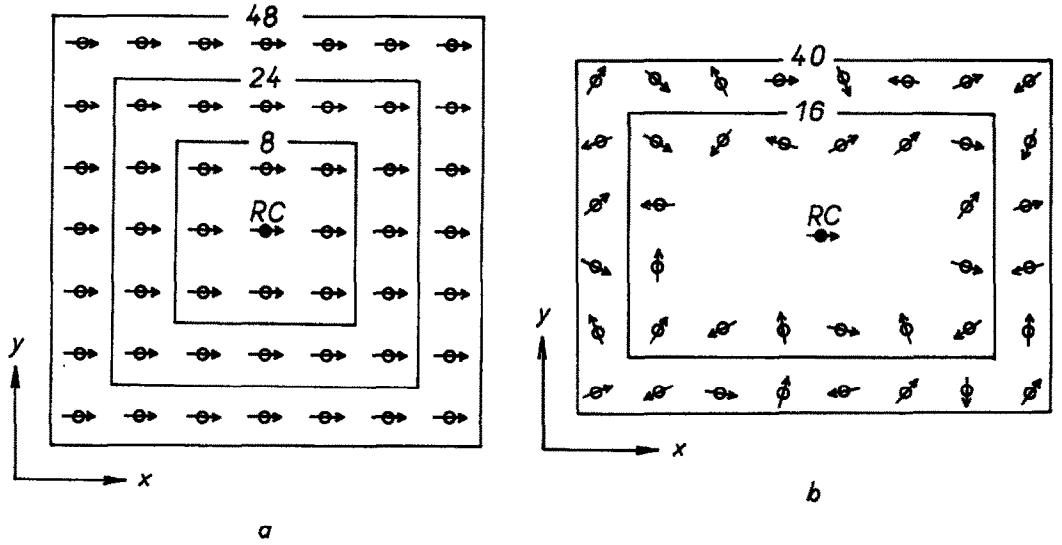

Fig. 2. Model of the antenna core surrounding the RC. (a) Antenna TDMs oriented along the x-axis for a RC with similar dimensions to those of the antenna (system 1 from table 1 is shown). Depending on the size of the system the number of antennas can be 8, 24 or 48. (b) Randomly oriented antenna TDMs in the xy-plane for the RC dimensions 6×3.6 nm estimated from X-ray data (system 12 from table 1 is shown). The number of antennas can be 16 or 40. ○, antenna; ●, reaction center; ↑, transition dipole moment.

lifetime $\tau=5$ ns [18]. For details see fig. 1 and refs. [7,11].

We investigate planar systems consisting of C678 antennas and a single P680 reaction center in the middle of the system. The transition dipole moment (TDM) of the RC is oriented along the x-axis. The antennas are arranged in one, two or three shells around the RC and form a regular "lattice" with a "lattice constant" $a=1.2$ nm (see fig. 2). The investigated antenna cores differ by the number of Chl molecules, the orientation of the antenna TDMs and the dimensions of the RC. The antenna TDMs are oriented (a) along the x-axis (systems 1–3, 10–11 in table 1), (b) along the y-axis (systems 4–6), (c) randomly in the xy-plane (systems 7–9, 12–13) or (d) randomly in space (system 14). We consider the following planar dimensions of the RC: (a) roughly the same as for the antennas (systems 1–9), similarly to refs. [4–7] and (b) 6×3.6 nm estimated [12] from X-ray analysis of the RC [13] (systems 10–14).

The supposed initial conditions correspond to the excitation by a very short x-polarized light pulse propagating along the z-axis. The probability of the occupation of the S_1 level of a given antenna or the RC at $t=0$ calculated in the dipole approximation [14] is proportional to $\cos^2\vartheta$, where ϑ denotes the angle between the TDM of the Chl molecule and the x-axis. Levels other than S_1 are not occupied at $t=0$. We assume the absorption of a single photon at $t=0$.

3. Solution of Pauli master equation

To describe the excitation energy transfer we use the Pauli master equation in the form

$$dP_i/dt=\sum_j F_{ij}P_j\,, \tag{1}$$

where $P_i(t)$ are the probabilities of occupation of the levels shown in fig. 1, F_{ij} denotes the rate constant for the transfer from the jth to ith level and $F_{ii}=-\sum_{j(\neq i)}F_{ji}$. For example, the rate constant F_{ij} for the transfer from the $j=S_1^{RC}$ to the $i=T_1^{RC}$ level is the intersystem crossing rate constant $k_1=1.34\times10^8$ s^{-1} (see fig. 1).

We solve the PME (1) numerically by expanding $P_i(t)$ as a power series by means of functions $\bar{J}_j(t)$ related to Bessel functions of the first kind $J_j(t)$,

$$\bar{J}_j(t)=(j+1)J_{j+1}(t)/t\,, \tag{2}$$

in the form

$$P_i(t)=\sum_j \Pi_{ij}\bar{J}_j(\beta t)\,. \tag{3}$$

Table 1

The systems investigated and their properties. Systems No. 1–9 correspond to a "small" RC shown in fig. 2a, No. 10–14 correspond to a "large" RC (fig. 2b). The orientation of the antenna TDMs is assumed to be along the x- or y-axis, random in the xy-plane or random in space. N is the number of antennas, t is the time from which the analytic solutions (5)–(8) may be used, τ_F^A, η_F^A are the lifetime and the quantum yield respectively of the antenna fluorescence at $t=0.5$ ns and η_{CT} is the quantum yield of the transfer to the CT level at $t=0.5$ ns. All the results were calculated with the accuracy given by the number of digits shown in the table

No.	Orientation of TDMs	N	t_0 (ps)	τ_F^A (ps)	η_{CT} (%)	η_F^A (%)
1	along x-axis	48	1.125	144.94	95	0.9
2	along x-axis	24	1.000	74.949	99	0.4
3	along x-axis	8	0.500	27.210	100	0.1
4	along y-axis	48	1.8	147	95	1.0
5	along y-axis	24	1.500	75.994	99	0.4
6	along y-axis	8	1.100	27.592	100	0.1
7	random in xy	48	1.800	145.11	95	1.0
8	random in xy	24	2.250	75.02	99	0.3
9	random in xy	8	1.525	27.241	100	0.1
10	along x-axis	40	3.000	133.49	97	0.9
11	along x-axis	16	3.500	56.434	99	0.4
12	random in xy	40	3.950	137.92	95	1
13	random in xy	16	3.950	59.49	99	0.3
14	random in space	40	7.5	203	92	1

Here, the Π_{ij} are the expansion coefficients and β is a time scaling factor. The advantage of this method is that the original differential kinetic equation (1) is transformed into a system of easily solvable recurrent matrix equations as described in refs. [15–17]. In our calculations, we used a 95-term expansion with $\beta = 1\times10^{14}\,s^{-1}$ (systems 10–14) or $2\times10^{14}\,s^{-1}$ (systems 1–9).

Because of the assumption of one absorbed photon at $t=0$ the intensities (I) and quantum yields (η) of the processes shown in fig. 1 are proportional to the probabilities $P_i(t)$. For example, the intensity of the antenna fluorescence is equal to the sum of the probabilities of occupation of the antenna S_1 levels multiplied by the corresponding rate constant, $I_F^A = k_F^A \sum_{i\in S_1^A} P_i$; the quantum yield of this process, η_F^A, is equal to the probability of occupation of the S_0 ($S_1^A \rightarrow S_0^A$) antenna level (see fig. 1). Similarly, the intensity of the RC fluorescence is proportional to the probability of occupation of the S_1^{RC} reaction center level, $I_F^{RC} = k_F^{RC} P_r$, $r = S_1^{RC}$; the quantum yield of the transfer to the CT level η_{CT} is equal to the probability of the occupation of this level.

Our numerical calculations showed that due to large intermolecular rate constants there is a time, t_0, of the order of a few picoseconds (see table 1), after which all the probabilities $P_i(t)$ of occupation of the S_1 antenna levels have – with a high accuracy – the same value. This means that $P_i(t) = I_F^A(t)/k_F^A N$; $i\in S_1^A$, N is the number of antennas. The formula for the time derivative of I_F^A, obtained from its definition, the PME (1) and the assumed values of F_{ij} (see fig. 1) can be written in the form

$$\mathrm{d}I_F^A/\mathrm{d}t = \{[k_F^{RC} + k_I + k_{CT} + F_{rr} - N(k_F^A + k_I)]/N\} I_F^A - [(k_F^{RC} + k_I + k_{CT} + F_{rr}) k_F^A / k_F^{RC}] I_F^{RC} .$$

Similarly, the rate of change of I_F^{RC} is given by

$$\mathrm{d}I_F^{RC}/\mathrm{d}t = -[(k_F^{RC} + k_I + k_{CT} + F_{rr})\, k_F^{RC}/N k_F^A]\, I_F^A + F_{rr} I_F^{RC} \qquad (4b)$$

These two coupled differential equations can easily be solved. The exact analytic solution of eqs. (4) for $I_F^A(t)$ and $I_F^{RC}(t)$ is a sum of two exponentials. One exponent, however, is about three orders of magnitude smaller than the other and the corresponding exponential may be neglected for $t > t_0$. The resulting approximate solution to eqs. (4) is

$$I_F^A(t) = I_F^A(t_0)\, \exp[-\alpha(t-t_0)] , \qquad (5a)$$

$$I_F^{RC}(t) = I_F^{RC}(t_0)\, \exp[-\alpha(t-t_0)] , \qquad (5b)$$

where

$$\alpha \equiv 1/\tau_F^A = [k_F^{RC} + k_I + k_{CT} + N(k_F^A + k_I)]/(N+1) \qquad (6)$$

and τ_F^A is the antenna fluorescence lifetime. Taking into consideration the values of the rate constants and assuming $N \lesssim 300$ we get with a high accuracy

$$\tau_F^A = (N+1)/k_{CT} . \qquad (7)$$

The kinetic equations for other observables can be derived from (1) in a similar manner. Those equations, which contain I_F^A and I_F^{RC} on their right-hand sides are solvable by the technique of successive integration. The results are as follows. The quantum yield of the transfer to the CT level

$$\eta_{CT}(t) = (k_{CT}/\alpha k_F^{RC})\, [I_F^{RC}(t_0) - I_F^{RC}(t)] + \eta_{CT}(t_0) , \qquad (8a)$$

the quantum yield of the RC fluorescence

$$\eta_F^{RC}(t) = (1/\alpha)\, [I_F^{RC}(t_0) - I_F^{RC}(t)] + \eta_F^{RC}(t_0) , \qquad (8b)$$

the intensity of the RC phosphorescence

$$I_P^{RC}(t) = -\{k_I k_P/[k_F^{RC}(\alpha - k_P)]\} I_F^{RC}(t) + \{I_P^{RC}(t_0) + \{k_I k_P/[k_F^{RC}(\alpha - k_P)]\} I_F^{RC}(t_0)\} \times \exp[-k_P(t-t_0)] , \qquad (8c)$$

the quantum yield of the RC phosphorescence

$$\eta_P^{RC}(t) = \{k_I k_P/[\alpha k_F^{RC}(\alpha - k_P)]\} [I_F^{RC}(t) - I_F^{RC}(t_0)] + \{I_P^{RC}(t_0)/k_P + k_I I_F^{RC}(t_0)/[k_F^{RC}(\alpha - k_P)]\} \times \{1 - \exp[-k_P(t-t_0)]\} + \eta_P^{RC}(t_0) , \qquad (8d)$$

the quantum yield of the antenna fluorescence

$$\eta_F^A(t)=(1/\alpha)[I_F^A(t_0)-I_F^A(t)]+\eta_F^A(t_0)\,, \tag{8e}$$

the intensity of the antenna phosphorescence

$$\begin{aligned} I_P^A(t) &= -\{k_1k_P/[k_F^A(\alpha-k_P)]\}I_F^A(t) \\ &+\{I_P^A(t_0)+\{k_1k_P/[k_F^A(\alpha-k_P)]\}I_P^A(t_0)\} \\ &\times\exp[-k_P(t-t_0)] \end{aligned} \tag{8f}$$

and the quantum yield of the antenna phosphorescence

$$\begin{aligned} \eta_P^A(t) &= \{k_1k_P/[\alpha k_F^A(\alpha-k_P)]\}[I_F^A(t)-I_F^A(t_0)] \\ &+\{I_P^A(t_0)/k_P+k_1I_F^A(t_0)/[k_F^A(\alpha-k_P)]\} \\ &\times\{1-\exp[-k_P(t-t_0)]\}+\eta_P^A(t_0)\,. \end{aligned} \tag{8g}$$

4. Discussion and conclusions

The most important conclusions that follow from this study are given below.

(1) Our numerical calculations have shown that in all the cases investigated there is a characteristic time, t_0, of the order of a few picoseconds (see table 1) which all S_1 antenna levels are occupied with the same probability. It follows from table 1 that t_0 increases with increasing number of antennas, N, increasing randomness of the orientation of the antenna transition dipole moments and increasing dimensions of the RC. The characteristic time, t_0, is in the range 0.5–7.5 ps.

(2) It has been shown that the same value for the probability of occupation of all S_1 antenna levels for $t>t_0$ allows us to find an analytic solution for the intensities and quantum yields of the processes shown in fig. 1. The analytic form of the results makes it possible to discuss the nature of the dependence of the observables on the rate constants and N. The intermolecular rate constants k, k', k'', ... do not appear in eqs. (5)–(8) so that the analytic results are independent of the Förster model and have more general validity. The only necessary assumption in this respect is that the intermolecular rate constants are a few orders of magnitude larger than the others.

(3) The quantum yields η_F^A, η_F^{RC} and intensities I_F^A, I_F^{RC} of the antenna and RC fluorescence, and the quantum yield of the transfer to the CT level η_{CT} have for $t>t_0$ a single-exponential form (see the discussion of eqs. (5)–(8)). It follows from eq. (6) that for $N\lesssim 300$ and the assumed values of the rate constants, the fluorescence lifetime is $\tau_F^A=(N+1)/k_{CT}$. The lifetime τ_F^A does not depend on the other rate constants. The measurements of τ_F^A for $t>t_0$ can be used to calculate N or k_{CT}. Using $k_{CT}=3.3\times10^{11}\ s^{-1}$ [7] and $\tau_F^A=492$ ps (Chlorella, dark adapted) given in table 3 of ref. [6], eq. (7) yields $N=161$. This is the number of Chl molecules in the long-wave form.

(4) The quantum yields η_P^A, η_P^{RC} and intensities I_P^A, I_P^{RC} have for $t>t_0$ a double-exponential form (see eqs. (8)) with corresponding lifetimes τ_F^A and $1/k_P$, k_P being the phosphorescence rate constant. It follows from the values of these lifetimes that the exponential with τ_F^A can be neglected for $t>200$ ps. Therefore, these observables for $t>200$ ps are single exponentials with lifetime $1/k_P$.

(5) The observables I_F^A, I_F^{RC}, I_P^A, I_P^{RC}, η_F^A, η_F^{RC}, η_P^A, η_P^{RC} and η_{CT} discussed in (3) and (4) depend on nine constants (the values of these quantities at $t=t_0$). These values reflect the concrete initial conditions and configuration of the system.

(6) It is obvious from the above discussion that the most significant information can be obtained from measurements for $t<t_0$. It is therefore desirable to perform experiments with a time resolution better than t_0.

(7) The parameter characterizing the efficiency of the transfer for different configurations of the photosynthetic unit is the quantum yield η_{CT}. The time evolution of η_{CT} for some typical systems investigated here for short times is shown in fig. 3. The values of η_{CT} are smaller than 2% for $t<t_0$. There are two reasons for this: (a) the occupation of the S_1 reaction center level from which the transfer to the CT level takes place is low and (b) the time t_0 is comparable with $1/k_{CT}$, the characteristic time of the transfer from the RC to the CT level. We see also that η_{CT} increases with increasing randomness of the orientation of the TDMs (compare 1 and 7; 10 and 12) with respect to that of the RC. The reason for this lies in the preferred absorption of light by the RC as

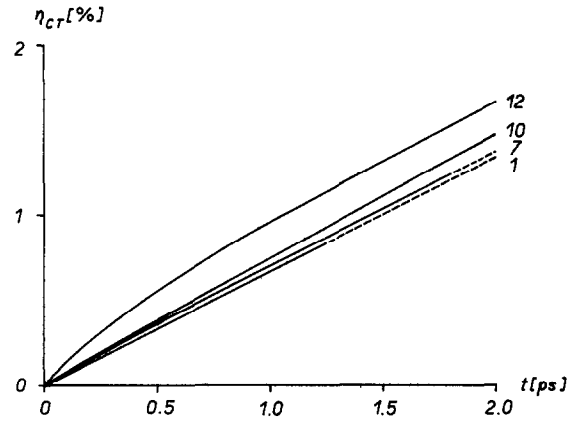

Fig. 3. Time dependence of the quantum yield η_{CT} of transfer to the CT level for systems 1, 7, 10 and 12 for short time. The results of numerical (full line) and analytical (eq. (8a) for $t > t_0$; dashed line) calculations are shown.

compared to antennas in our systems. The same explanation is valid for the decrease of η_{CT} with increasing N. We see from table 1 (system 1–14), however, that η_{CT} at $t=0.5$ ns is very high and does not depend (within experimental error) on the initial conditions and the configuration of the photosynthetic unit. The time after which η_{CT} changes negligibly follows from eqs. (5)–(8a), $t \gg t_0$.

(8) The quantum yield, η_F^A, characterizing the radiative losses by antenna fluorescence (η_F^A for $t=0.5$ ns, see table 1) is very low ($\leqslant 1\%$). Since, in our model, $k_1 = 2k_F^A$, it can be calculated approximately from $\eta_F^A = \frac{1}{3}(100 - \eta_{CT})$.

(9) The intensity of the antenna fluorescence, I_F^A, for short time is shown in fig. 4. In systems in which absorption by the RC is preferred with respect to the antennas, I_F^A increases initially and then decreases (compare 7 and 12 with 1 and 10). We see that the effect of the initial conditions and configuration of the system on I_F^A is most significant for $t < t_0$.

(10) It follows from table 1 and the form of the analytic solution that the dimensions of the RC have for $t > t_0$ a very small effect on the efficiency of the transfer (η_{CT}).

Most of the conclusions given above are related to the large ratio of the intermolecular/intramolecular rate constants. The most significant assumptions of our model are the Förster prescription for the intermolecular rate constants and the use of the incoherent kinetic equation (PME), the modelling of the antenna core by the regular lattice of single chlorophyll a molecules, the neglect of transfer among the T_1 states of the pigment molecules and the assumed form of the initial excitation. Because of these assumptions, an experimental examination of our conclusions is necessary. We believe, however, that most of the conclusions have general validity.

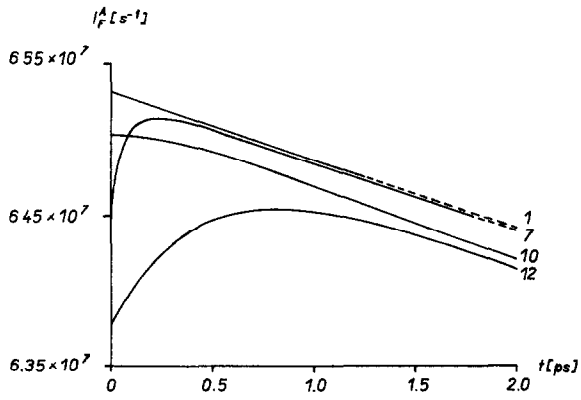

Fig. 4. Time dependence of the intensity of fluorescence I_F^A from the antenna core for systems 1, 7, 10 and 12 for short time. The results of numerical (full line) and analytical (eq. (5a) for $t > t_0$; dashed line) calculations are shown.

Acknowledgement

The authors would like to thank Professor A.Yu. Borisov (Moscow State University), Professors K. Vacek, L. Valenta and Dr. P. Pancoska (Charles University, Prague) for stimulating discussions.

References

[1] R.K. Clayton, Photosynthesis – physical mechanisms and chemical patterns (Cambridge Univ. Press, Cambridge, 1980).
[2] C. Sybesma, ed., Advances in photosynthesis research, (Nijhoff, The Hague, 1984).
[3] F.K. Fong, ed., Light path of photosynthesis (Springer, Berlin, 1982).
[4] G.R. Seely, J. Theor. Biol. 40 (1973) 173, 189.
[5] Z.G. Fetisova, A.Yu. Borisov and M.V. Fok, J. Theor. Biol. 112 (1985) 41.

[6] G.S. Beddard and R.J. Cogdell, in: Light path of photosynthesis, ed. F.K. Fong (Springer, Berlin, 1982) p. 46.
[7] L.L. Shipman, Photochem. Photobiol. 31 (1980) 157.
[8] G. Paillotin, C.E. Swenberg, J. Breton and N.E. Geacintov, Biophys. J. 25 (1979) 513.
[9] V.M. Kenkre, in: Energy transfer in condensed matter, ed. B. di Bartolo (Plenum Press, New York, 1984).
[10] T. Förster, in: Modern quantum chemistry, Istanbul Lectures, Part 3, ed. O. Sinanoğlu (Academic Press, New York, 1965).
[11] V. Kapsa, Thesis, Charles University, Prague (1985).
[12] P. Pancoska, private communication.
[13] J. Deisenhofer, O.Epp, K. Miki, R. Huber and H. Michel, J. Mol. Biol. 180 (1984) 385.
[14] D. Bohm, Quantum theory (Prentice-Hall, Englewood Cliffs, 1952).
[15] L. Skala and O. Bilek, Acta Univ. Carolinae Pragensis, Math. Phys. 23 (1982) 61.
[16] L. Skala and O. Bilek, Phys. Stat. Sol. 114b (1982) K51.
[17] L. Skala, Intern. J. Quantum Chem. 23 (1983) 497.
[18] A. Yu. Borisov, private communication.